

Thermodynamic variational method for liquid alloys with chemical short-range order

A. Pasturel* and J. Hafner

Institut für Theoretische Physik, Technische Universität Wien, Karlsplatz 13, A-1040 Wien, Austria

P. Hicter

*Laboratoire de Thermodynamique et Physico-Chimie Métallurgiques, Ecole Normale Supérieure d'EEG,
Domaine Universitaire, Boîte Postale No. 75, F-38402 Saint-Martin d'Hères, France*

(Received 23 April 1985)

We present a first-principles study of chemical short-range ordering in liquid (*s,p*)-bonded alloys. Our approach is based on an optimized pseudopotential technique for the construction of the interatomic potentials and a thermodynamic variational technique based on the Gibbs-Bogoliubov inequality and hard-sphere Yukawa reference potentials (we use the analytical solution of the mean spherical solution for the equal-diameter case). The analysis of the redistribution of the valence electrons upon alloying allows us to elucidate the electronic origin of the ordering potential. In the case of a moderately strong ordering interaction, the application of the Gibbs-Bogoliubov variational technique yields a reasonably accurate prediction of the structure factors and of the thermodynamic excess functions. For very strong ordering potentials, a free minimization of the variational upper bound to the exact free energy gives unrealistic results. This is a consequence of the complete decoupling of number-density and concentration fluctuations in the mean-spherical approximation to the equal-diameter hard-sphere Yukawa mixture. We find that realistic solutions may be found by imposing the condition that the exact and the reference-system ordering potentials be the same at the mean effective atomic diameter. This constrained minimization of the variational free energy yields good results for the structure factors, but rather bad ones for the thermodynamic excess functions. We are able to show that this is due to a neglect of the finite electronic mean free path of the electrons in those concentration regions where it is comparable to the mean interatomic distance.

I. INTRODUCTION

Over the last decade the formation of chemical short-range order (CSRO) in liquid metallic alloys has been a subject of increasing attention. Numerous systems exhibiting this effect have been discovered and studied (see Refs. 1 and 2 for recent reviews).

A theoretical treatment of CSRO in liquid alloys clearly involves two distinct steps: (i) the determination of the interatomic forces from an electronic theory of chemical bond, and (ii) the calculation therefrom of the structure and of the thermodynamic properties using the methods of the classical theory of liquids.

To date the only reliable scheme for obtaining the interatomic interactions in metallic systems is based on the linear response of the conduction electrons to the electron-ion potential, which is valid only in systems whose ions scatter the electrons weakly and are describable by pseudopotentials (see Heine and Weaire³ for a review). For the pure simple metals, the theory has now been developed to a point where the pair potentials derived from the optimized pseudopotentials based on orthogonalized-plane-wave expansions of the conduction-electron states⁴ (the optimization serves to minimize the importance of the higher-order perturbation contributions) and those derived from the effective potential approach⁵ yield convergent answers which may be considered reliable and accurate.^{6,7} The situation is more difficult in alloys, the main problems being the transferabili-

ty of the electron-ion pseudopotentials and the short mean free path of the conduction electrons due to the strong disorder scattering.

To calculate the structure of a liquid mixture, we could, in principle, proceed in three different ways: (i) by computer simulation, (ii) by solving one of the integral equations of the theory of liquids (see, e.g. Ref. 8), and (iii) by using thermodynamic perturbation theory. Even with present-day computers, the simulation of binary liquid mixtures goes to the very limits of the computational capacity. Consequently, only a very few liquid metallic alloys have been investigated,^{9,10} and the authors are aware only of a single attempt to simulate a system with strong CSRO.¹¹ The problem of solving the system of three coupled integral equations representing the alloy has not even been tackled yet. This leaves us with thermodynamic perturbation theory as the only tractable alternative.

The most elementary form of thermodynamic perturbation theory is the variational method based on the Gibbs-Bogoliubov inequality.¹² The exact free energy F of a system is always smaller than the free energy F_0 of a reference system plus the expectation value of the perturbation (i.e., the difference between the exact interatomic interactions Φ and those of the reference system, Φ_0), evaluated with the distribution functions of the reference system,

$$F \leq F_0 + \langle \Phi - \Phi_0 \rangle . \quad (1)$$

If the reference system depends on one or more param-

ters, it is hence possible to establish an upper bound to the exact free energy by minimizing the right-hand side of (1) as a function of these parameters.

For alloys with a nearly ideal mixing behavior, a variational treatment with a mixture of hard spheres of different diameters as a reference system has met with considerable success,^{13,14} but such an approach is certainly unable to cope with ordering phenomena.

Copstake *et al.*¹⁵⁻¹⁷ have shown that the structural manifestations of ordering in molten salts, liquid semiconductors, and even liquid metallic alloys may be modeled using a mixture of hard spheres all having the same diameter, but opposite charges, and interacting through a Coulomb or screened Coulomb (Yukawa) potential. For such a reference system, an analytical solution of the mean spherical approximation is available.¹⁸ Very recently, the present authors have shown^{19,20} that, combined with a very simple treatment of the electronic contributions to the free energy of a liquid alloy, this model may be used to fit the thermodynamic excess functions and partial static structure factors of a large series of Li- and Na-based alloys with polyvalent and noble metals with good success.

This opens the way to a thermodynamic variational treatment of liquid alloys with CSRO. In the present paper we present the first such calculation. Our approach is based on interatomic potentials derived from the optimized first-principles pseudopotentials introduced earlier by one of us,²¹ and applied successfully to a number of crystalline,²² liquid,^{14,23} and amorphous alloys.²³ In Sec. II we recapitulate briefly the derivation of the interatomic pair potentials.

The properties of the reference system (mixture of hard spheres with equal diameters and Yukawa interactions) are summarized in Sec. III.

In Sec. IV we present an application of this new variant of the variational technique to systems with a weak to moderate CSRO (Mg-Zn, Mg-Li). In that case it is possible to determine a true upper bound to the exact free energy by minimizing the right-hand side of (1) as a function of the hard-sphere diameter σ , the strength of the ordering potential at contact ϵ , and the screening constant κ .

In Sec. V we turn to the more difficult case of strongly ordering systems. Here it turns out that there is no real minimum in the approximate expression for the free energy within the physically realistic range of the model parameters. This is related to the fact that the conditions that have to be imposed to the hard-sphere-Yukawa (HSY) system in order to enable one to find an analytical solution (equality of the HS diameters, charge neutrality) yield to a complete decoupling of number-density and concentration fluctuations. In the context of the variational method we find that a physically realistic solution may be found by imposing the condition $\Phi_{CC}(\sigma) = -\epsilon$, i.e., by requiring that the strength of the model (HSY) ordering potential at contact ϵ is just equal to the exact ordering potential $\Phi_{CC}(R)$ evaluated at $R = \sigma$. This condition introduces the necessary coupling between density and concentration fluctuations. An application is illustrated at the example of the structure of liquid Li-Pb alloys.

Section VI summarizes what we believe we have achieved: we have presented the first attempt to calculate ordering phenomena in liquid alloys from first principles, without any adjustable parameters. Pseudopotential theory is found to provide a reasonably realistic description of the ordering interaction, and allows to relate the strength and the form of the ordering potential to a redistribution of the conduction-electron densities. That pseudopotential theory is applicable even in cases where the differences in valence are as large as in Li-Pb might appear surprising, and we emphasize that at the present stage the theory should be regarded as semiquantitative at best. Many points, such as, for example, the influence of the short mean free path of the conduction electrons in the strong scattering regime on the screening function, remain to be investigated.

II. INTERATOMIC POTENTIALS IN ALLOYS

One of the stumbling blocks on our way to a clear understanding of the interatomic potentials in alloys is the problem of the transferability of the electron-ion pseudopotential. The naive approximation which considers the bare pseudopotential as fixed and accounts only for changes in the linear screening functions with the mean conduction-electron density is suited only for systems with a rather small difference in the electron density of the components. Evidently, the pseudopotential is a collective rather than an atomic property: it describes the scattering of conduction electrons by an ionic core within a given surrounding medium. If that changes (e.g., by alloying), the pseudopotential changes too. The approach introduced earlier by one of us²¹ represents the most direct attack on this problem: Instead of designing the pseudopotential as to optimize its transferability (see, e.g., Refs. 24 and 25), the bare pseudopotentials for the constituents of a binary alloy are constructed anew for each concentration and carefully optimized (using the Cohen-Heine²⁶ criterion of the smoothest possible wave function) for that specific composition. As a consequence, the bare ionic pseudopotentials of the alloy constituents will now be concentration dependent.

As the technical details of the construction of the pseudopotential have been well documented in earlier publications,^{14,21-23} we shall not repeat them here. We will merely discuss the interrelation between charge rearrangements and the concentration-dependent changes in the interatomic pair potentials.

In a simplified way, we might view the formation of a binary simple-metal alloy as follows: the starting point is a homogeneous electron gas with a density $n_0 = Z/\Omega$ corresponding to the mean atomic volume Ω in the alloy and the average valence $Z = (1-c)Z_A + cZ_B$ (c is the concentration of the B atoms), into which the A and B ions are introduced as a perturbation. According to the Pauli principle, the conduction-electron states must be orthogonal to the orbitals of the ionic cores: to those of type A on the sites occupied by A ions, and to those of type B on the sites occupied by the B ions. The orthogonality constraint reduces the probability of finding a conduction electron in the region of an ion core—in the language of

pseudopotential specialists one usually says "the ion forms an orthogonalization hole." The important point is the following. If the alloy is formed by metals with very different electron densities, one species of ions (say the A ions) "sees" a much larger electron density than in the pure metal. Consequently, it has to form a larger orthogonalization hole, whereas that around the B ion will be smaller in the alloy than in the pure metal. These changes in the orthogonalization-hole charges are compiled in Table I; a reduced orthogonalization-hole charge also reflects a reduced strength of the repulsive part of the pseudopotential and vice versa.

In the second step we calculate the linear response of the conduction electron to the pseudopotential of the ion plus the orthogonalization hole. Ion core, orthogonalization hole, and screening charge altogether form the electrically neutral pseudoatom. Of course, the form of the screening charge around a given atom will again be different in the alloy and in the pure metal. This is illustrated in Fig. 1 at the example of the screening charge density around a Li ion in pure Li and equiatomic alloys of Li with Na, Mg, Al, and Pb. So, in fact what happens is a competition between two electron-transfer mechanisms: First, we are transferring electrons from A to B , from the low-electron-density to the high-electron-density component, i.e., in the direction expected from the electronegativity difference. In the second step the electrons are allowed to respond to the external perturbation and they do so by redistributing themselves as to minimize potential gradients and so to minimize the ground-state energy. Partly, this is achieved by accumulating electrons in the core region of the ion with the increased orthogonalization hole charge (Fig. 1). In fact, a very early discussion of these two competing electron-transfer mechanisms associated with the electronegativity and the electroneutrality principles can be found in Pauling.²⁷

We expect that the orthogonalization effect will influence mainly the electrostatic part of the effective interatomic potentials, whereas the change in the screening charges affects mainly the indirect ion-electron-ion interaction, which dominates the form of the interatomic interactions around the nearest-neighbor distance. Figure 2 shows that this is indeed the case: the interatomic potentials follow the redistribution of the screening. As the screening charge around the Li ions is drawn closer to the

TABLE I. Orthogonalization-hole charges (per ion) in some Li-based binary alloys and in the pure metals.

	Li n_{OH}	X n_{OH}
Li	0.0622	
Na		0.0730
Li-Na	0.0465	0.0856
Mg		0.1500
Li-Mg	0.0895	0.1140
Al		0.2108
Li-Al	0.1439	0.1345
Pb		0.4197
Li-Pb	0.1402	0.3223

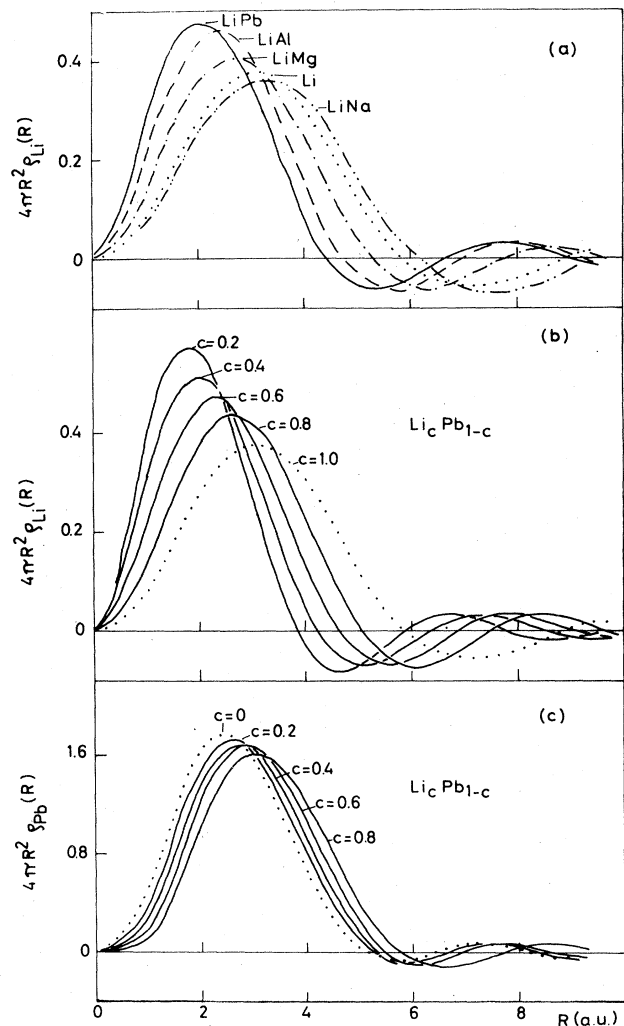


FIG. 1. (a) Screening charge distribution $\rho_{Li}(R)$ around a Li ion in pure Li (\cdots), and equiatomic alloys of Li with Na ($-\cdots-$), Mg ($-\cdot-\cdot-$), Al ($- - -$), and Pb ($—$). (b) Screening charge distribution $\rho_{Li}(R)$ around a Li ion in a series of Li_cPb_{1-c} alloys. (c) Screening charge distribution $\rho_{Pb}(R)$ around a Pb ion in a series of Li_cPb_{1-c} alloys.

core with increasing valence of the other component, the repulsive core of the effective pair potential $\Phi_{Li-Li}(R)$ shrinks due to a reduced overlap, and its first attractive minimum is shifted to smaller distances. This is, in fact, an effect which is well known in physical metallurgy under the name of the "chemical compression" upon alloying with a more electronegative metal, the effective diameter of the more electropositive atom is reduced.²⁸

For large distances all three pair potentials oscillate in phase as we would expect, since it is the Fermi-momentum which sets the wavelength of the oscillations. The amplitude of the oscillations is set by the magnitude of the pseudopotential matrix element at the Fermi surface. As the pseudopotential of the polyvalent ions is less effectively screened in the alloy because of the reduced electron density, the oscillations in the pair interactions between these ions will become more pronounced. In Li-

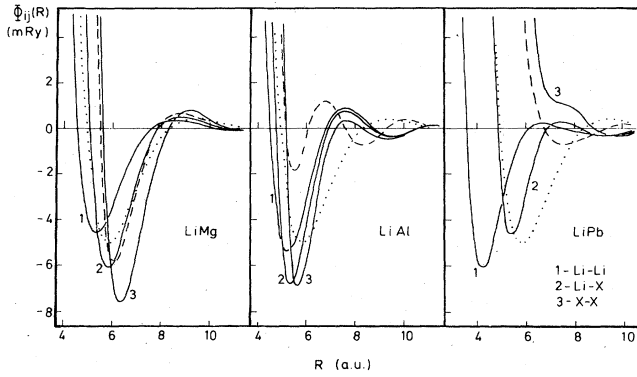


FIG. 2. Effective interatomic pair potentials $\Phi_{ij}(R)$ in equiatomic alloys of Li with Mg, Al, and Pb, calculated for the experimentally known density of the liquid alloys at a temperature close to $T=1000$ K. The solid lines give the pair interactions in the alloys, the dotted line that pair potential in pure Li, and the dashed lines the pair potentials in pure Mg, Al, and Pb, all calculated again at the densities of the liquid metals at $T=1000$ K.

Mg and Li-Al this results in a very deep minimum in $\Phi_{Mg-Mg}(R)$ and $\Phi_{Al-Al}(R)$, respectively, around the nearest-neighbor distance. In Li-Pb a repulsive hump appears at the edge of the repulsive part of $\Phi_{Pb-Pb}(R)$, because the oscillations are now much more pronounced than in pure Pb. However, the minimum at the nearest-neighbor distance is still covered by the repulsive core (for a recent discussion of the interplay of repulsive and oscillatory interactions in determining the form of the effective pair potential, see Hafner and Heine.²⁹

We also note that with increasing difference in valence, the interaction between unlike atom pairs is no longer simply the mean value of the $A-A$ and $B-B$ interactions, and the minimum in $\Phi_{AB}(R)$ is now much deeper than in a simple set of additive pair interactions. However, it is not only the relative depth of AA , BB , and AB potentials which determines the strength of the ordering potential: the size difference is equally important. Here it is appropriate to transform from the individual particle interactions $\Phi_{AA}(R)$, $\Phi_{BB}(R)$, and $\Phi_{AB}(R)$ to the pair potentials

$$\Phi_{NN}(R) = c_A^2 \Phi_{AA}(R) + c_B^2 \Phi_{BB}(R) + 2c_A c_B \Phi_{AB}(R), \quad (2a)$$

$$\Phi_{CC}(R) = c_A c_B [\Phi_{AA}(R) + \Phi_{BB}(R) - 2\Phi_{AB}(R)], \quad (2b)$$

$$\Phi_{NC}(R) = 2c_A c_B [c_A \Phi_{AA}(R) - c_B \Phi_{BB}(R) + (c_B - c_A) \Phi_{AB}(R)], \quad (2c)$$

representing, in turn, an average pair interaction (which couples to the fluctuations in the mean number density), an ordering interaction (coupling to the concentration fluctuations), and a cross term. For the three equiatomic alloys Li-Mg, Li-Al, and Li-Pb these potentials are shown in Fig. 3. Figure 4 shows their variation with concentration at the example of a series of Li-Pb alloys.

Note that a $\Phi_{CC}(R)$ that is positive around the nearest-neighbor distance d_1 expresses the fact that the interaction between unlike-atom pairs is stronger than in an average like-atomic pair—thus a positive $\Phi_{CC}(d_1)$ will induce

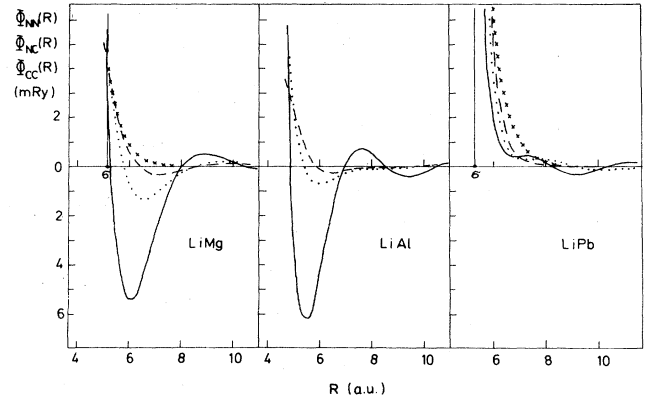


FIG. 3. Effective pair potentials $\Phi_{NN}(R)$ (—), $\Phi_{NC}(R)$ (\cdots), and $\Phi_{CC}(R)$ (---), describing the coupling between density and concentration fluctuations in equiatomic Li-Mg, Li-Al, and Li-Pb alloys. The vertical line marks the effective hard-sphere diameter σ , the crosses the reference ordering potential $\Phi_{CC}^{HSY}(R)$ derived from the variational condition (see Secs. III and IV).

a tendency to heterocoordination. Note that for larger distances the ordering interaction is very strongly damped—this is simply a consequence of the fact that asymptotically all three pair interactions have to oscillate

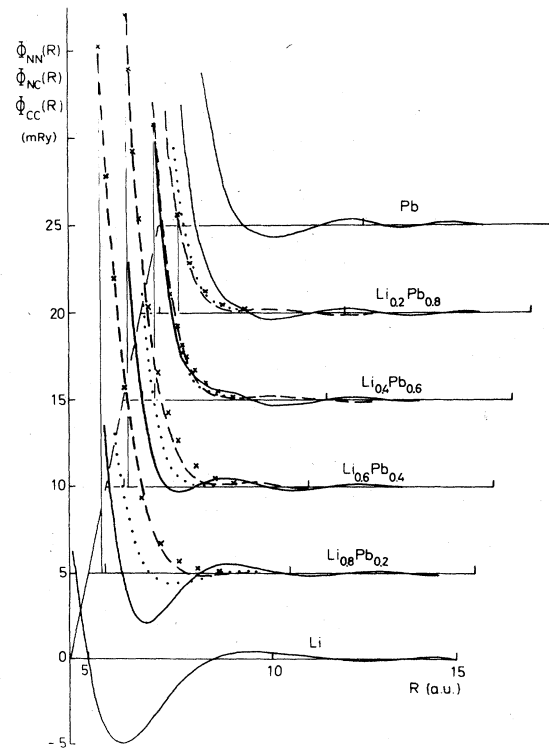


FIG. 4. Effective pair potentials $\Phi_{NN}(R)$ (—), $\Phi_{NC}(R)$ (\cdots), and $\Phi_{CC}(R)$ (---), for Li-Pb alloys as a function of concentration. The thin vertical lines mark the effective hard-sphere diameter σ and the crosses show the reference ordering potential $\Phi_{CC}^{HSY}(R)$ determined by the variational condition (see Sec. V).

in phase. This will be an important point in the following thermodynamic variational calculations. The strength of the ordering potential essentially scales with the importance of the charge-transfer effects, but—as can be seen by comparing Li-Mg and Li-Al—size effects are also important. The concentration-dependent variation of the potentials in the series of $\text{Li}_c\text{Pb}_{1-c}$ alloys shown in Fig. 4 demonstrates that the ordering effects are by no means symmetric with respect to concentration; the ordering effect is strongest at the composition $\text{Li}_{0.8}\text{Pb}_{0.2}$. From Figs. 1(b) and 1(c) it can be seen that this is precisely the composition with the minimal overlap between unlike pairs of pseudoatoms.

Thus we find that optimized pseudopotential theory describes reasonably well the trends in the interatomic interactions, which we expect on the basis of the known structural and thermodynamic properties. In addition, it allows to relate the origin of the ordering potential to a spatial redistribution of the conduction electrons. The important point is that the ordering potential is not really of electrostatic origin, but—because of the long-range cancellation effects described above—it has an approximate screened Coulomb form for the distances of interest. Thus it will be amenable to a perturbation treatment based on a hard-sphere—Yukawa—type reference system.

Of course, this section does not present an exhaustive discussion of the electronic origin of chemical short-range order (which must be left to future work), but it appears legitimate to say that we have now an adequate working knowledge of the fundamental chemical interactions.

III. THE HARD-SPHERE—YUKAWA MODEL

A. The analytical solution of the mean-spherical approximation for the HSY model

The mean-spherical approximation (MSA) for a binary mixture of hard spheres with Yukawa tails is defined by the Ornstein-Zernike equations

$$h_{ij}(R) = c_{ij}(R) + \sum_k n_k \int c_{ik}(|\mathbf{R}-\mathbf{R}'|) h_{kj}(R') d^3R' \quad (3)$$

in connection with the closure relations

$$c_{ij}(R) = -\beta\Phi_{ij}(R) = -\beta Q_i Q_j e^2 \exp[-\kappa(R-\sigma)]/R, \quad R > \sigma_{ij} \quad (4a)$$

$$h_{ij}(R) = -1, \quad R < \sigma_{ij} \quad (4b)$$

for the total correlation functions $h_{ij}(R) = g_{ij}(R) - 1$ and

$$c_{CC}(R) = \begin{cases} -\frac{\beta\epsilon\omega}{x} \left[\frac{1-\exp(-Zx)}{Z} + \omega \frac{\cosh(Zx)-1}{2Z^2\exp(Z)} \right], & x > 1 \\ \beta\epsilon \exp[-Z(x-1)]/x, & x < 1 \end{cases} \quad (11)$$

with $x = R/\sigma$. The Fourier transform of the direct correlation function is then given by

$$c_{CC}(q) = \frac{4\pi\beta\epsilon}{q} A_1 \left[\frac{1-\cos(q\sigma)}{q} - \frac{q}{\kappa^2+q^2} \right] + A_2 \frac{\exp(-\kappa Z)[\kappa \sin(q\sigma) + q \cos(q\sigma)]}{\kappa^2+q^2} - A_3 \left[\frac{\kappa \sinh(Z)\sin(q\sigma) - q \cosh(Z)\cos(q\sigma)}{\kappa^2+q^2} \right], \quad (12)$$

the direct correlation. If all spheres have the same diameter ($\sigma_{AA} = \sigma_{BB} = \sigma_{AB} = \sigma$) and if the charge-neutrality condition

$$c_A Q_A + c_B Q_B = 0 \quad (5)$$

is respected, one finds that after transforming to the Bhatia-Thornton³⁰ functions,

$$c_{NN}(R) = c_A^2 c_{AA}(R) + c_B^2 c_{BB}(R) + 2c_A c_B c_{AB}(R),$$

$$c_{NC}(R) = c_A c_B [c_{AA}(R) + c_{BB}(R) - 2c_{AB}(R)], \quad (6)$$

$$c_{CC}(R) = c_A c_{AA}(R) - c_B c_{BB}(R) + (c_B - c_A) c_{AB}(R),$$

describing the spatial correlation of fluctuations in the number density n and in the concentration, the system of three coupled integral equations [(3) and (4)] reduces to two independent equations,¹⁸

$$h_{NN}(R) = c_{NN}(R) + n \int c_{NN}(|\mathbf{R}-\mathbf{R}'|) h_{NN}(R') d^3R', \quad (7a)$$

$$c_{NN}(R) = 0, \quad R > \sigma \quad (7b)$$

$$h_{NN}(R) = -1, \quad R < \sigma \quad (7c)$$

and

$$h_{CC}(R) = c_{CC}(R) + n \int c_{CC}(|\mathbf{R}-\mathbf{R}'|) h_{CC}(R') d^3R', \quad (8a)$$

$$c_{CC}(R) = -\beta\Phi_{CC}(R)$$

$$= -\beta c_A c_B \Delta Q^2 e^2 \exp[-\kappa(R-\sigma)]/R$$

$$= \beta\epsilon\sigma \exp[-\kappa(R-\sigma)]/R, \quad R > \sigma \quad (8b)$$

$$h_{CC}(R) = 0, \quad R < \sigma. \quad (8c)$$

The third equation has the trivial solution

$$\Phi_{NC}(R) = h_{NC}(R) = c_{NC}(R) = 0. \quad (9)$$

Equation (7) is identical to the Percus-Yevick equation for hard spheres, and hence we know analytical solutions for the thermodynamic functions and for the direct correlation functions.³¹ Equation (8) has been solved analytically by Waisman.¹⁸ He showed that the result may be expressed in terms of a parameter ω which is the solution of the quartic equation

$$\beta\epsilon\eta = \frac{\omega\{Z - \omega/[2\exp(Z)]\}}{12\{1 + \omega[1 - \exp(-Z)]/2Z\}^4} \quad (10)$$

(η is the hard-sphere packing fraction, $\eta = \frac{1}{6}n\pi\sigma^3$, and $Z = \kappa\sigma$). The direct correlation function $c_{CC}(R)$ is given by

with

$$\begin{aligned} A_1 &= \frac{\omega}{\kappa} \left[\frac{\omega}{2Z \exp(Z)} - 1 \right], \\ A_2 &= \sigma \exp(Z) - \omega/\kappa, \\ A_3 &= \omega^2/\kappa Z \exp(Z). \end{aligned} \quad (13)$$

The static structure factor is simply

$$S_{CC}(q) = c_A c_B [1 - n c_{CC}(q)]^{-1}.$$

The analytic expressions for c_{NN} (in real and reciprocal space) and

$$S_{NN}(q) = [1 - n c_{NN}(q)]^{-1}$$

are well known³² and need not be repeated here. Analytical expressions for the thermodynamic functions may be derived using the coupling-constant formalism,¹⁸ with the final result¹⁹

$$F^{\text{HSY}} = \frac{3}{2} k_B T + \Delta H_{\text{ord}} - T(S_{\text{HS}} + \Delta S_{\text{ord}}). \quad (14)$$

S_{HS} is the hard-sphere entropy (we use the expression proposed by Carnahan and Starling,³³ and

$$\begin{aligned} \Delta H_{\text{ord}} &= 2\pi n \int g_{CC}(R) \Phi_{CC}(R) R^2 dR \\ &= -\frac{1}{2} \omega \epsilon \end{aligned} \quad (15)$$

and

$$\Delta S_{\text{ord}} = [f(\omega) - f(0)]/2\eta \quad (16)$$

are the contributions to the enthalpy and entropy of formation associated with a nonvanishing ordering potential. Equation (15) shows that ω is just twice the ratio between the ordering enthalpy and the strength of the ordering potential at contact. The function $f(\omega)$ is given by

$$f(\omega) = -\frac{B_1 + B_2\omega + B_3\omega^2}{72B_4^2(1 + B_4\omega)^3}, \quad (17)$$

with

$$\begin{aligned} B_1 &= Z \left[\frac{2}{\exp(Z) - 1} - 1 \right], \\ B_2 &= -\frac{3}{2} [1 - 3 \exp(-Z)], \\ B_3 &= \exp(-Z) [1 - \exp(-Z)]/4Z, \\ B_4 &= [1 - \exp(-Z)]/2Z. \end{aligned} \quad (18)$$

Equations (10)–(18) represent the fully analytic representation of the HSY reference system needed in the variational calculation. However, before we explicitly formulate the variational condition, we think that it is necessary to investigate relative roles of charge and screening on the thermodynamic properties and on the atomic structure.

B. The influence of charge and screening upon the properties of a HSY system

It is clear that as the screening constant κ changes from 0 to ∞ , the interatomic potential changes gradually from

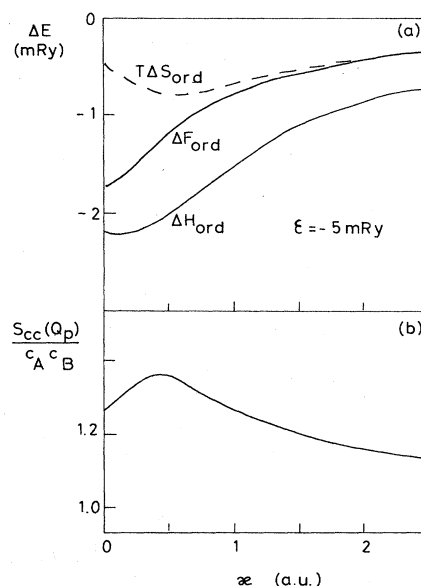


FIG. 5. (a) Variation of the heat, entropy, and free energy of formation, and (b) of the height of the main peak in the structure factor $S_{CC}(q)$, with the screening constant κ . The strength of the ordering interaction and packing fraction are kept constant, $\epsilon = -5$ mRy, $\eta = 0.40$, and $T = 1000$ K.

a pure Coulombic to a pure hard-sphere form. In the former limit the model is expected to represent an ionic melt [in that context it is usually called the restricted primitive model³⁴ (RPM)], where the latter limit is known to yield a good first description of liquid metals and rare gases. The vast intermediate range is still relatively unexplored, except for a recent study of Holzhey *et al.*³⁵ on the variations of the atomic structure with charge and screening constant. We have found it worthwhile to extend their study in a systematic way.

In Figs. 5 and 6 we show the variation of the heat, en-

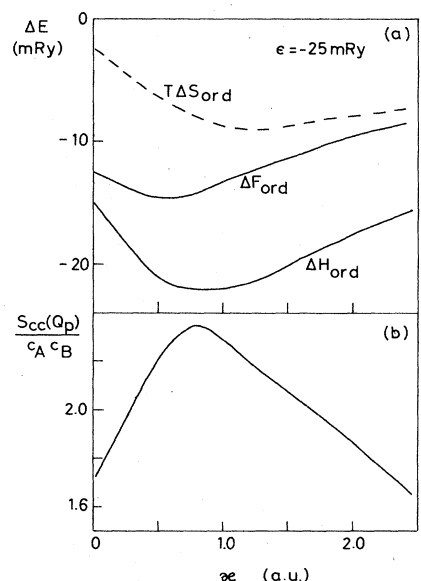


FIG. 6. As for Fig. 5, but for $\epsilon = -25$ mRy.

ropy, and free energy of formation, and of the height of the first peak in the concentration-fluctuation structure factor $S_{CC}(Q_p)$ with the screening constant κ at different values of ϵ and at constant $\eta=0.40$, $T=1000$ K. The first somewhat surprising result is that the strength of the ordering effects does not vary monotonically with the screening. The maximum degree of ordering does not occur for the pure Coulombic case, but at a finite value of the screening parameter whose value increases even with the strength of the ordering interaction. Furthermore, ΔH_{ord} , ΔS_{ord} , and ΔF_{ord} are all extremal at different values of the screening parameter. This is essentially a consequence of the fact that the ordering process is dominated by the short-range interaction: Once the ordering potential is strong enough to produce the maximum short-range ordering (where each atom is surrounded essentially only by unlike atoms), a further decrease of the

screening constant will only strengthen the interaction with the second-nearest neighbors (which will be predominantly like atoms) and can only decrease the total ordering energy. This is illustrated in Fig. 7. In part (a) we show the ordering potential $\Phi_{CC}(R)$ at a fixed $\epsilon=-25$ mRy for different values of the screening parameter: $\kappa=0.1$ a.u. corresponds to a nearly Coulombic interaction, $\kappa=0.7$ a.u. to the maximum value of $S_{CC}(Q_p)$ and the minimum in ΔH_{ord} (cf. Fig. 6), $\kappa=1.3$ a.u. to the strongest effect in ΔS_{ord} , and $\kappa=1.9$ a.u. to a very strongly screened interaction.

It is a rather striking coincidence that the strongest effect in the structure and enthalpy show up if the ordering potential extends just out to the second-nearest neighbors ($R/\sigma=2$), and that the strongest effect on the entropy is seen when $\Phi_{CC}(R)$ extends only to the first minimum in the pair-correlation function (i.e., $R/\sigma\sim 1.5$). We have

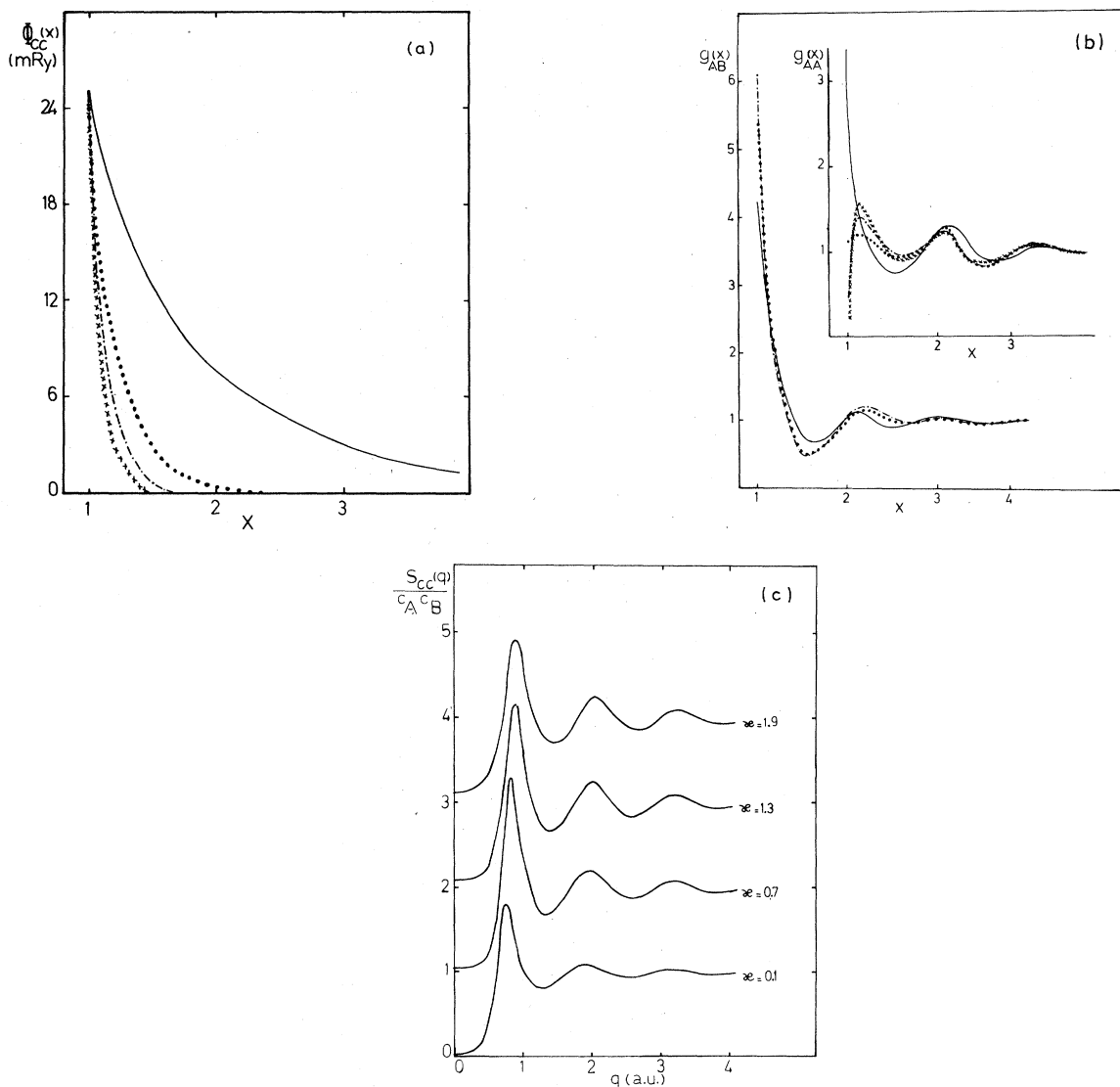


FIG. 7. Variation of (a) the ordering potential $\Phi_{CC}(R)$, (b) the pair-correlation functions $g_{AA}(R)=g_{BB}(R)$ and $g_{AB}(R)$, and (c) the concentration-fluctuation structure factor $S_{CC}(q)$, with the screening constant κ (—, $\kappa=0.1$; ····, $\kappa=0.7$; -·-·-·, $\kappa=1.3$; $\times\times\times\times\times\times\times$, $\kappa=1.9$) at a fixed strength of the ordering interaction at contact, $\epsilon=-25$ mRy, $\eta=0.40$, and $T=1000$ K.

verified that this correlation holds for other choices of the parameters and of the concentration as well. The variation of the pair-correlation functions and of the structure factor with the screening constant is rather surprising as well [Fig. 7(b)]: the value of the unlike-atom pair-correlation function at contact first increases with concentration, but essentially saturates beyond $\kappa=1.3$ a.u.; the form of $g_{AB}(R)$ is nearly independent of κ for $\kappa > 1.3$ a.u. The like-atom correlation function shows the more interesting effects: The value at hard contact first decreases dramatically with increasing κ ; at $\kappa=0.7$ a.u., $g_{AA}(R)=g_{BB}(R)$ shows only weak fluctuations even at small distances. At an even stronger screening, the value at contact continues to decrease (showing that direct contacts are increasingly prohibited), but a distinct peak appears near $R/\sigma=1.15$. This shows that although *direct* contacts are even more strongly suppressed in a screened as opposed to a Coulombic system, rather *close* contacts are allowed once the screening is sufficiently strong. These effects are also reflected in the concentration-fluctuation structure factor: Judging from the height of the first peak, $S_{CC}(Q_p)$, the ordering effect is about equally strong at $\kappa=0.1$ a.u. and at $\kappa=1.9$ a.u. The difference is in the higher-order oscillations—they are strongly damped in the nearly Coulombic case, and rather strong in the screened case, reflecting the more pronounced structure in the like-atom correlations.

This shows that within the HSY system the correlation between “ionicity” and ordering is not as clear as one would have thought. At a fixed value of the strength of the interaction at contact, screening is not detrimental to ordering: The introduction of a certain degree of screening even enforces ordering effects by suppressing unfavorable interactions with more distant neighbors. With our definition of the Yukawa interactions [Eq. (8b)], constant ϵ means also constant Q_1, Q_2 . However, the screening part might also be rewritten in the form $(\Delta Q')^2 \exp(-\kappa R)$, allowing the screening to penetrate into the hard core. In that case, a variation of κ at constant ϵ would also mean a drastic variation of the charges Q'_1, Q'_2 . The problem is only that, within the $\Phi_{CC}(R)$ necessary to explain the observed ordering phenomena, the charges Q'_i would be unrealistically large (see the discussion in Refs. 19, 20, and 49), and that the notion of a screening penetrating the “hard” core would be difficult to interpret in a physically realistic way. Therefore we had good reasons to adopt the convention (8b).

C. The variational expression for the free energy

With the reference-system free energy and correlation functions given by Eqs. (10)–(18), the appropriate form of the Giggis-Bogoliubov inequality (1) reads (we use now atomic units)

$$F \leq \bar{F}(\eta, \epsilon, \kappa) = \frac{3}{2} k_B T + E_{FE} + E_{BS} + E_{es} - T[S_{HS}(\eta) + \Delta S_{ord}(\eta, \epsilon, \kappa)]. \quad (19)$$

In (19) the band-structure energy is given by

$$E_{BS} = \frac{1}{2\pi^2 n} \sum_{i,j=A,B} (c_i c_j)^{1/2} \int F_{ij}(q) S_{ij}^{HSY}(q; \eta, \epsilon, \kappa) q^2 dq \quad (20a)$$

$$= \frac{1}{2\pi^2 n} \int [F_{NN}(q) S_{NN}^{HS}(q, \eta) + F_{CC}(q) S_{CC}^{HSY}(q; \eta, \epsilon, \kappa)] q^2 dq, \quad (20b)$$

with the partial-energy-wave-number characteristics $F_{ij}(q)$, which are just the Fourier transforms of the indirect ion-electron-ion part of the pair interaction $\Phi_{ij}(R)$. The electrostatic energy is expressed in the form

$$E_{es} = \sum_{i,j=A,B} (c_i c_j)^{1/2} Z_i Z_j \frac{2}{\pi} \int [S_{ij}^{HSY}(q; \eta, \epsilon, \kappa) - \delta_{ij}] dq \quad (21a)$$

$$= \bar{Z}^2 \frac{2}{\pi} \int [S_{NN}^{HS}(q; \eta) - 1] dq + (\Delta Z)^2 \frac{2}{\pi} \int [S_{CC}^{HSY}(q; \eta, \epsilon, \kappa) - c_A c_B] dq. \quad (21b)$$

Note that $\bar{Z} = c_A Z_A + c_B Z_B$ and $\Delta Z = Z_A - Z_B$; E_{FE} , the “free-electron” energy, contains the zeroth- and first-order contributions and is independent of the structure of the alloy; for its explicit form see Ref. 14.

Alternatively, (19) might be written in real space as

$$\bar{F}(\eta, \epsilon, \kappa) = \frac{3}{2} k_B T + E_0 + E_p - T[S_{HS}(\eta) + \Delta S_{ord}(\eta, \kappa, \epsilon)], \quad (22)$$

with the pair-interaction energy

$$E_p = 2\pi n \sum_{i,j=A,B} c_i c_j \int g_{ij}^{HSY}(R; \eta, \kappa, \epsilon) \Phi_{ij}(R) R^2 dR \quad (23a)$$

$$= 2\pi n \int [g_{NN}^{HS}(R; \eta) \Phi_{NN}(R) + g_{CC}(R; \eta, \epsilon, \kappa) \Phi_{CC}(R)] R^2 dR. \quad (23b)$$

E_0 consists of the free-electron energy and the structure-insensitive self-interaction terms contained in (20) and (21); after some cancellation it turns out that E_0 is just the sum of the electron-gas energy and of the electrostatic interactions of the ions with their own screening clouds.³⁶

For the computational point of view, Eqs. (20b) and (21b) are most convenient. The integrals in the expression for the band-structure energy (20b) are rapidly convergent, and the electrostatic energy (21b) can be obtained in closed form. For the one-component hard-sphere fluid this result was derived by Jones,³⁷

$$\int [S_{NN}^{\text{HS}}(q; \eta) - 1] dq = 2\pi^2 n \sigma^2 \lim_{t \rightarrow 0} [H_{NN}(t) - 1/t^2] = \frac{1 - \eta/5 - \eta^2/10}{1 - 2\eta}, \quad (24)$$

where σ is the hard-sphere diameter and $H_{NN}(t)$ is the Laplace transform of the direct correlation function $h_{NN}(R)$ —it applies in our case to the number-density-fluctuation contribution. The analogous result for the concentration-fluctuation part,

$$\int [S_{CC}^{\text{HSY}}(q; \eta, \epsilon, \kappa) - c_A c_B] dq = c_A c_B 2\pi^2 n \sigma^2 \lim_{t \rightarrow 0} H_{CC}(t), \quad (25)$$

is somewhat lengthy—the result and derivation are given in the Appendix.

In the spirit of the Gibbs-Bogoliubov inequality, the optimal HSY parameters are determined through the variational conditions

$$\left. \frac{\partial \bar{F}(\eta, \epsilon, \kappa)}{\partial \eta} \right|_{T, n, \epsilon, \kappa} = 0, \quad (26a)$$

$$\left. \frac{\partial \bar{F}(\eta, \epsilon, \kappa)}{\partial \epsilon} \right|_{T, n, \eta, \kappa} = 0, \quad (26b)$$

$$\left. \frac{\partial \bar{F}(\eta, \epsilon, \kappa)}{\partial \kappa} \right|_{T, n, \eta, \epsilon} = 0, \quad (26c)$$

which determine the HSY parameters as a function of density and temperature. As a consequence of the variational conditions (26), the entropy is simply given by

$$S = - \left[\frac{\partial F}{\partial T} \right]_{n, \eta, \epsilon, \kappa} - \left[\frac{\partial F}{\partial \eta} \right]_{n, T} \left[\frac{\partial \eta}{\partial T} \right]_n - \left[\frac{\partial F}{\partial \epsilon} \right]_{n, T} \left[\frac{\partial \epsilon}{\partial T} \right]_n - \left[\frac{\partial F}{\partial \kappa} \right]_{n, T} \left[\frac{\partial \kappa}{\partial T} \right]_n = S_{\text{HS}}(\eta) + \Delta S_{\text{ord}}(\eta, \epsilon, \kappa) \quad (27)$$

because the second, third, and fourth terms vanish according to (26).

IV. SYSTEMS WITH WEAK CHEMICAL SHORT-RANGE ORDER

We begin by studying systems with a rather weak tendency for chemical short-range ordering, for which the approximations inherent in our model (first of all a size ratio close to one!) should be reasonably well satisfied. The first alloy selected was Mg_7Zn_3 —for this system both neutron- and x-ray diffraction experiments have been performed in the liquid³⁸ and in the amorphous states.^{39,40} As the neutron-scattering lengths are nearly equal, the neutron data are insensitive to CSRO, but the x-ray data show a distinct prepeak indicative of a pronounced CSRO.^{38,39} The pair potentials for this alloy shown in Fig. 8 demonstrate that this system is indeed ideally suited for the HSY variational method: $\Phi_{NC}(R)$ is very close to zero for all distances. At $T=673$ K and $n=0.00649$ a.u.³, the result of the variational calculation is $\eta=0.51$, $\epsilon=-2.60$ mRy, and $\kappa=2.3$ a.u.⁻¹. This packing fraction corresponds to a hard-sphere diameter of $\sigma=5.31$ a.u. This is exactly the value for which

$$\Phi_{NN}(\sigma) - \Phi_{\min} = \frac{3}{2} k_B T \quad (28)$$

[Φ_{\min} is the minimum value of $\Phi_{NN}(R)$]. This simple rule^{14,36} expresses the fact that σ is just an average collision distance. The ordering potential corresponding to these values of ϵ and κ is also shown in Fig. 8—we find that indeed the variationally determined models the exact ordering potential very closely. Figure 9 shows the partial

structure factors $S_{NN}(q)$ and $S_{CC}(q)$, calculated at two different temperatures; as one would intuitively expect, the CSRO is strongly temperature dependent. The composite (x-ray-weighted) static structure factor is given by

$$S(q) = \{ \langle f(q) \rangle^2 S_{NN}(q) + [\Delta f(q)]^2 S_{CC}(q) \} / \langle f(q)^2 \rangle, \quad (29)$$

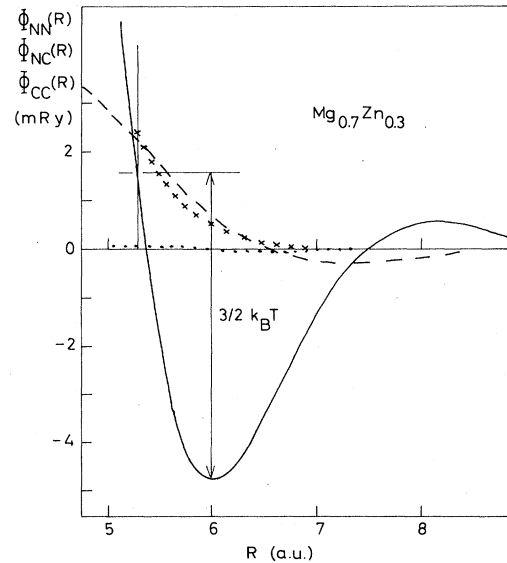


FIG. 8. Pair potentials $\Phi_{NN}(R)$ (—), $\Phi_{NC}(R)$ (· · · ·), and $\Phi_{CC}(R)$ (— — —), for a liquid Mg_7Zn_3 alloy at $T=673$ K. The vertical line marks the effective hard-sphere diameter σ , the crosses show the variationally determined model-ordering potential $\Phi_{CC}^{\text{HSY}}(R)$.

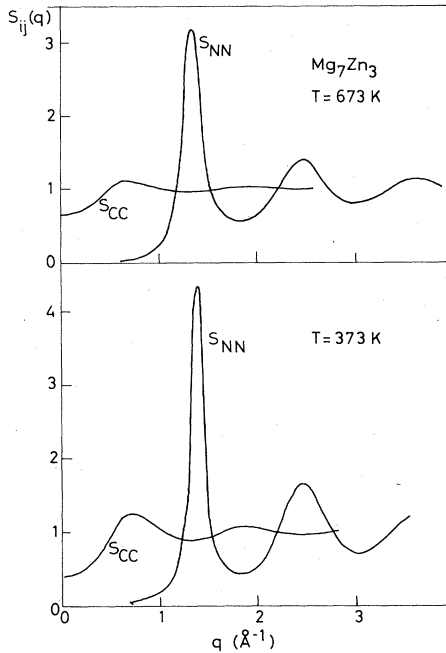


FIG. 9. Partial structure factors $S_{NN}(q)$ and $S_{CC}(q)$ for liquid ($T=673$ K) and supercooled liquid ($T=373$ K) Mg_7Zn_3 alloys.

with $\langle f \rangle = c_A f_A + c_B f_B$ and $\Delta f = f_A - f_B$; the $f_i(q)$ are the x-ray-scattering form factors (the Fourier transforms of the valence-electron densities). $S(q)$ for liquid and amorphous Mg_7Zn_3 alloys is shown in Fig. 10, for the amorphous phase $S_{NN}(q)$ was taken from an earlier cluster-relaxation calculation,⁴¹ and $S_{CC}(q)$ was approximated by that of a supercooled liquid at $T=373$ K, i.e.,

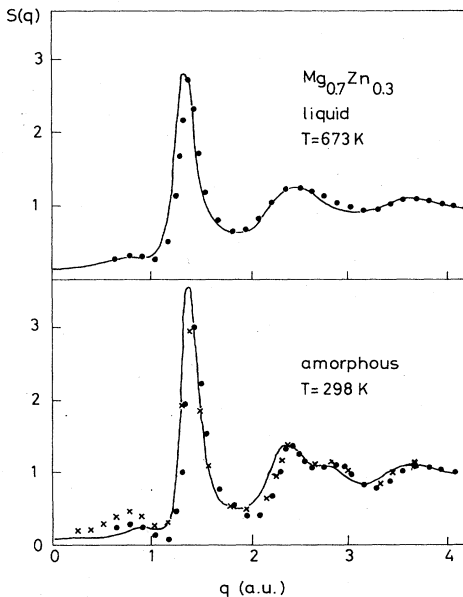


FIG. 10. Composite (x-ray-weighted) static structure factor for liquid ($T=673$ K) and amorphous (room-temperature) Mg_7Zn_3 alloy. Solid lines, calculated; solid circles (Ref. 38) and crosses (Ref. 39), x-ray-diffraction results.

close to the glass-transition temperature. In comparing theory and experiment, we have to remember that the contribution of $S_{CC}(q)$ to the composite structure factor is only 18% in this alloy. The observed agreement between theory and experiment is quite good, except that the separation between prepeak and main peak is weaker than found in the experiment. This might point to a slight underestimate of the ordering potential.

The next system studied is liquid Li-Mg: the difference in the atomic volumes is small, so that the HSY model should be applicable. However, in this case $\Phi_{NC}(R)$ is not small compared to $\Phi_{CC}(R)$ (see Fig. 3). The variational conditions (26) have a well-defined solution, and again the variationally determined HSY parameters correspond exactly to those derived from Eq. (28), and

$$\Phi_{CC}(\sigma) = -\epsilon \quad (30)$$

(see Fig. 3 for a detailed comparison of the exact and reference-system interactions for an equiatomic Li-Mg alloy). Li-based alloys offer a peculiar advantage for structural studies: Because of the negative neutron-scattering length of ${}^7\text{Li}$ ($b_{\text{Li}} = -0.2337$ and $b_{\text{Mg}} = 0.52$), there exists a composition (the "zero alloy") for which the neutron-diffraction experiment measures directly $S_{CC}(q)$.⁴² In the Li-Mg system the zero-alloy is $\text{Li}_{0.7}\text{Mg}_{0.3}$; the calculated and the measured $S_{CC}(q)$ are given in Fig. 11. Keeping in mind that this is an *ab initio* calculation, with the density of the alloy⁴³ as the only input, the achieved agreement can certainly be considered as quite encouraging. Next we look at the thermodynamic excess functions. The free enthalpy ΔG , the enthalpy ΔH , and the entropy ΔS of formation are shown in Fig. 12. The agreement achieved for the heat of formation is as good as we can reasonably expect it to be.

The calculated entropy of formation is distinctly too low, even if we keep in mind that the experimental ΔS is calculated from ΔH and ΔG referring to slightly different temperatures and, hence, is probably an overestimate. The dominant contribution to the calculated ΔS comes from the change in the HS entropy (Fig. 12); thus the moderate agreement with experiment is probably to be blamed on the interatomic potentials (it appears that they overestimate the chemical compression effect slightly) as well as on the neglect of the density-concentration cross correlation (even a small size mismatch would give a positive contribution to ΔS). Taken altogether we find that

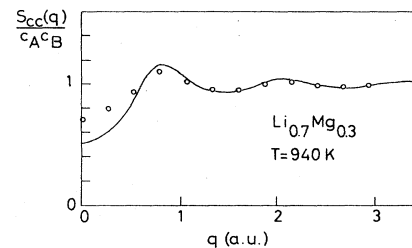


FIG. 11. Concentration-fluctuation structure factor $S_{CC}(q)$ for the "zero alloy" $\text{Li}_{0.7}\text{Mg}_{0.3}$ at $T=940$ K. Solid line, theory; open circles, neutron-diffraction experiment (after Ref. 42).

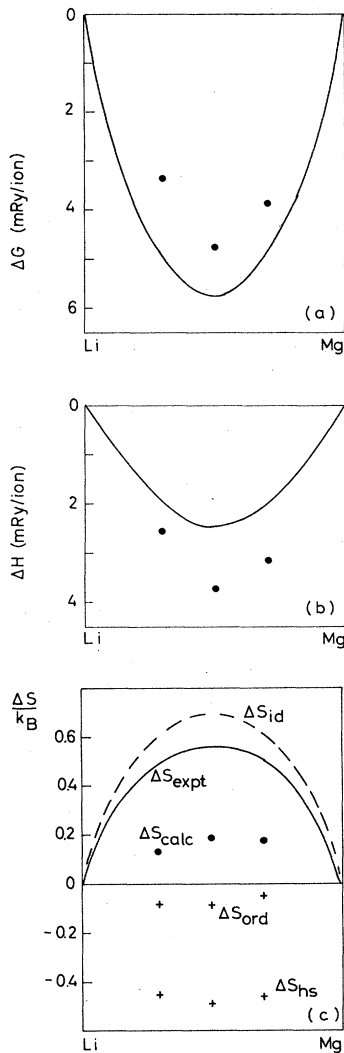


FIG. 12. (a) Free enthalpy ΔG , (b) enthalpy ΔH , and (c) entropy of formation ΔS of liquid Li-Mg alloys. Solid circles, theory ($T=940$ K); solid lines, experiment [ΔH from Sommer (Ref. 44), $T=940$ K, and ΔG from Saboungi (Ref. 45), $T=870$ K, with ΔS calculated from these two results]. The crosses give the calculated ordering and packing (ΔS_{ord} and ΔS_{HS} , respectively) contributions to the entropy of formation.

for weakly ordering systems the HSY variational method combined with the optimized pseudopotential technique yields quite encouraging results.

V. SYSTEMS WITH STRONG CHEMICAL SHORT-RANGE ORDER

The ordering potential in Li-Pb alloys is about 5 times stronger than in Li-Mg alloys; thus we would expect the ordering phenomena to be much more manifest in this system. The straightforward application of the variational conditions (the calculations are performed for $T=1000$ K and the experimental densities of Ruppertsberg and Speicher⁴⁶) yields a disappointing result: there is no minimum in the free energy within the physically realistic

range of parameters. The total free energy continues to decrease into the direction of very small effective hard-sphere diameters σ and very large ordering interactions ϵ . Thus it appears that the loss in energy from the mean interparticle repulsions is insufficient to counterbalance the energy gain from the ever-increasing ordering potential, and that the difficulties arise from the complete decoupling of the number-density and concentration fluctuations, which is an artifact of the MSA-HSY model. Numerical solutions of the hypernetted-chain equations by Copestake *et al.*¹⁷ for both hard-core and soft-core Yukawa particles and molecular-dynamics simulations by Jacucci *et al.*¹¹ for the same system have shown that even in the equal-diameter case the NC cross correlation is non-negligible, once the ordering potential is strong enough. However, we find that we arrive at a physically acceptable solution if we impose the additional constraint $\Phi_{CC}(\sigma) = -\epsilon$ [see Eq. (30)], so that the variational conditions now read

$$\left. \frac{\partial \bar{F}(\eta, \epsilon, \kappa)}{\partial \eta} \right|_{n, T, \epsilon, \kappa} = 0, \quad (31a)$$

$$\left. \frac{\partial \bar{F}(\eta, \epsilon, \kappa)}{\partial \kappa} \right|_{n, T, \eta, \kappa} = 0, \quad (31b)$$

$$\Phi_{CC}(\sigma) = -\epsilon. \quad (31c)$$

The resulting reference-system interactions are again compared with the exact pair potentials in fig. 4, Eq. (28) is well obeyed, and the variationally determined screening

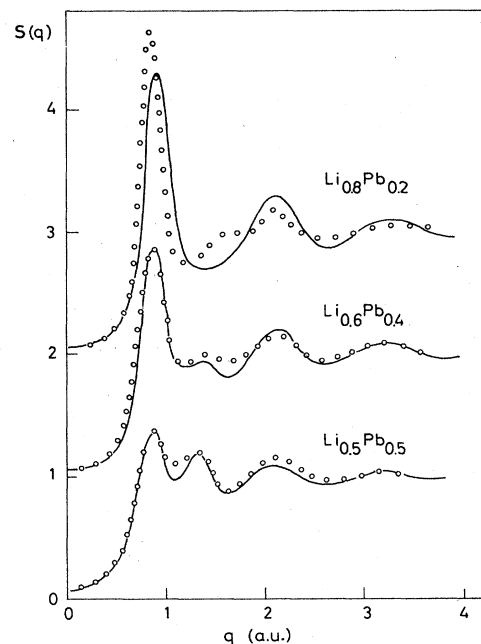


FIG. 13. Composite (neutron-weighted) static structure factor $S(q)$ for several liquid $\text{Li}_c\text{Pb}_{1-c}$ alloys at $T=1000$ K. The alloy $\text{Li}_{0.80}\text{Pb}_{0.20}$ is very close to the composition of the zero alloy, so that $S(q)$ is essentially identical to $S_{CC}(q)/c_A c_B$; for larger Pb concentrations there is an increasing contribution from $S_{NN}(q)$. Solid lines, theory; open circles, neutron-diffraction results of Ruppertsberg and Reiter (Ref. 47).

TABLE II. Input data (concentration c and mean atomic volume Ω), variationally determined model parameters (η , packing fraction; σ , hard-sphere diameter; κ , screening constant; ϵ , strength of the ordering potential at hard contact), and entropy contributions (S_{gas} , ideal-gas entropy; S_{HS} , hard-sphere entropy; ΔS_{ord} , ordering entropy) for liquid $\text{Li}_c\text{Pb}_{1-c}$ alloys.

c	Ω (a.u.)	η	σ (a.u.)	κ (a.u.)	ϵ (mRy)	S_{gas}/k_B	S_{HS}/k_B	$\Delta S_{\text{ord}}/k_B$
0.9	156.7	0.36	4.76	1.40	-20.2	10.86	-2.57	-0.94
0.8	149.6	0.42	4.93	1.80	-30.2	11.32	-3.42	-1.90
0.7	156.6	0.43	5.04	1.70	-30.2	11.76	-3.59	-2.01
0.6	165.5	0.44	5.18	1.7	-27.0	12.44	-3.76	-1.582
0.5	176.3	0.44	5.29	1.7	-20.9	13.01	-3.76	-1.037
0.4	187.7	0.43	5.35	1.9	-15.7	13.58	-3.59	-0.65
0.3	197.5	0.42	5.43	1.9	-10.2	14.14	-3.50	-0.26

^aAfter Ruppertsberg and Speicher, Ref. 46.

constant reproduces the form of $\Phi_{CC}(R)$ rather well (see also Table II).

The calculated static structure factors for a series of liquid $\text{Li}_c\text{Pb}_{1-c}$ alloy are shown in Fig. 13 and are compared with experiment—the agreement with experiment is surprisingly good. However, if we turn to the thermodynamic properties, we find that the calculated entropies are much too low. (Experimental values for ΔS in Li-Pb alloys may be found in the paper by Saboungi *et al.*⁴⁸) This concerns both the packing term ΔS_{HS} and the ordering contribution ΔS_{ord} . The discrepancy is too large to be attributed to the neglect of size effects. It seems that the pair interactions derived from the pseudopotential calculations overestimate both the effective hard-core diameter (thus it appears that the chemical-compression effect is rather underestimated in the case of Li-Pb) and the strength of the ordering potential. A comparison with our earlier model calculations (where we had fitted the HSY-type ordering potential to the experimental heat of formation) points to an overestimate of σ of up to 3% (corresponding to a change in S_{HS} of about $0.5k_B$) and to an overestimate of the parameter ω (depending on both ϵ and κ). Ruppertsberg and Schirmacher⁴⁹ have attempted to construct an “experimental” ordering potential by inverting the MSA equation (8). The result corresponds again quite closely to a Yukawa form, with the parameters $\epsilon = -20$ mRy and $\kappa = 0.58$ a.u. for $\text{Li}_{0.8}\text{Pb}_{0.2}$. This would suggest (see Table II) that our ordering potentials have about the right magnitude at contact, but that the screening is too weak. Ruppertsberg and Schirmacher argue that the small value of the screening constant is related to a reduced density of states at the Fermi level compared to the free-electron value.

In fact, the comparison of our calculated structure factor with experiment also indicates that our potentials are too strongly screened, at least in the Li-rich range. This can be deduced from the amplitude of the higher-order oscillations in $S_{CC}(q)$ (cf. the discussion at the end of Sec. II B): they are overestimated in our calculation for Li concentrations $c_{\text{Li}} > 0.5$. This is precisely the region where the electrical resistivity is very large,⁵⁰ so that the mean free path of the electrons is of the order of magnitude of the interatomic distances. Within our formalism, the main effect of the short electronic mean free path is to change the screening function (see, e.g., de Gennes⁵¹): the singularity in the Lindhard function is smeared out and

this ultimately yields a damping of the Friedel oscillations in the screening charge distribution and in the interatomic interactions. However, as we have learned that the decay of the ordering potential depends strongly upon the compensation of the oscillations in the individual interatomic interactions, the resulting effect on the ordering potential $\Phi_{CC}(R)$ is not so easily predicted.

VI. CONCLUSIONS

We present the following:

(1) The optimized first-principles pseudopotentials may be used to construct ordering potentials in (s,p)-bonded alloys. For systems with small differences in electron density and/or valence, the predictions are quantitatively accurate. For systems with a large difference in valence, the predictions are rather semiquantitative in character: the strength of ordering potential is predicted with a seemingly reasonable accuracy, but the screening is certainly overestimated. The most urgent correction to be introduced seems to be the effect of the short electronic mean free path upon the screening function.

(2) The HSY system is an interesting reference system for modeling chemical short-range order. However, the variation of the strength of the ordering effects with screening is not monotonic, as one might expect on the basis of plausibility arguments. We find that at a fixed strength of the ordering potential at hard contact, the ordering effects are strongest if the screening is just strong enough to restrict the ordering interaction to the nearest-neighbor shell. For a weaker screening, the interactions with the second-nearest neighbors start to reduce the ordering effects.

(3) The HSY system can serve as a reference system for a Gibbs-Bogoliubov thermodynamic variational calculation in chemically ordering liquid alloys. For systems with a relatively weak ordering effects and small size differences, the optimal reference system parameters may be determined by a free minimization of the upper bound to the exact free energy.

(4) In more strongly ordering systems, the neglect of the cross correlation between number-density and concentration fluctuations (which is an artifact of the equal-diameter HSY model) yields to physically unrealistic results for a free minimization of the upper bound to the free energy. In that case we found it necessary to impose

the condition $\Phi_{CC}(\sigma) = -\epsilon$, which guarantees that the strength of the ordering potential at the effective mean atomic diameter is the same for the reference and for the exact potentials. In the example of Li-Pb alloys, we show that the constrained variational method yields surprisingly accurate results for the structure factor, but rather disappointing ones for the thermodynamic excess functions. Our detailed study of the HSY system allows us to conclude that this is to be blamed on an overestimate of the screening constant in the Li-rich region, where the electronic mean free path is of the order of magnitude of the interatomic distance.

To summarize, the combined application of the optimized pseudopotential technique and of the HSY thermodynamic variational method seems to be a promising approach to chemical short-range order in liquid alloys. In the limit of very strong ordering interactions, corrections for electronic-mean-free-path effects are necessary.

ACKNOWLEDGMENTS

This work has been supported by the Fonds zur Förderung der wissenschaftlichen Forschung in Österreich (Austrian Science Foundation) under Project No. 5486. One of us (A.P.) thanks the Centre National de la Recherche Scientifique (CNRS) for a leave of absence.

APPENDIX: ANALYTIC CALCULATION OF THE ORDERING CONTRIBUTION TO THE ELECTROSTATIC ENERGY OF THE HSY SYSTEM

The ordering contribution to the electrostatic energy is given by

$$H_{CC}(t) = \frac{F(t) + \frac{\beta P}{\sigma} \frac{1}{Z+t} + \frac{\omega}{2te^Z} \left[\frac{\beta P/\sigma}{Z-t} - \frac{\beta P/\sigma}{Z+t} \right]}{1 - 12\eta \frac{1}{t} \left[F(-t) - F(t) + \frac{\beta P/\sigma}{Z-t} - \frac{\beta P/\sigma}{Z+t} \right]}, \quad (\text{A7})$$

with

$$P = \epsilon \exp(Z), \quad Z = \kappa\sigma \quad (\text{A8})$$

and

$$F(t) = \int e^{-tx} f(x) dx, \quad x = R/\sigma \quad (\text{A9})$$

$$F(R) = c_{CC}(R) + \beta \Phi_{CC}(R).$$

The parameter ω is given by the solution of Eq. (10); $c_{CC}(R)$ is given by Eq. (11). Thus we have all the necessary information to calculate $H_{CC}(t)$ and to take the limit $t \rightarrow 0$. After a lengthy calculation we find

$$\alpha_{CC} = \frac{24\beta\epsilon\eta}{\sigma} \frac{\frac{\omega}{Z} \left[\frac{1}{\omega} - 1 - \frac{1}{Ze^Z} - \frac{\omega}{2Z} \left[\frac{1}{e^Z} + \frac{1}{2Ze^Z} - \frac{1}{2Z} \right] \right]}{1 + 12\beta\epsilon\eta(\omega/Z)D(\omega, Z)}, \quad (\text{A10})$$

with

$$D(\omega, Z) = \left[1 - \frac{2}{Z^2} + \frac{2}{Ze^Z} \left[1 + \frac{1}{Z} \right] \right] - \frac{\omega}{Z} \left[\frac{1}{2e^Z} - \frac{1}{Z^2 e^Z} - \frac{1}{2Z} \left[1 - \frac{1}{Z} \right] + \frac{1}{2Ze^{2Z}} \left[1 + \frac{1}{Z} \right] \right] - \frac{1}{\omega} \left[1 + \frac{1}{Z} \right]. \quad (\text{A11})$$

$$\Delta E_{es} = (\Delta Z)^2 \frac{2}{\pi} \int [S_{CC}^{\text{HSY}}(q; \eta, \epsilon, \kappa) - c_{AC}c_B] dq. \quad (\text{A1})$$

To calculate the integral in (A1), we note that the concentration-fluctuation correlation function $h_{CC}(R)$ is given by

$$\int [S_{CC}(q) - c_{AC}c_B] q \sin(qR) dq = 2\pi^2 n c_{AC}c_B h_{CC}(R). \quad (\text{A2})$$

A Laplace transformation of (A2) yields

$$\int [S_{CC}(q) - c_{AC}c_B] q \frac{q}{(t/\sigma)^2 + q^2} dq = 2\pi^2 n \sigma^2 c_{AC}c_B H_{CC}(t), \quad (\text{A3})$$

with

$$H_{CC}(t) = \int e^{-tx} x h_{CC}(x) dx, \quad x = R/\sigma. \quad (\text{A4})$$

Thus the electrostatic ordering energy may be written in the form

$$\Delta E_{es} = c_{AC}c_B (\Delta Z)^2 \alpha_{CC}, \quad (\text{A5})$$

with

$$\alpha_{CC} = \frac{1}{c_{AC}c_B} \frac{2}{\pi} \int [S_{CC}(q) - c_{AC}c_B] dq = 4\pi n \sigma^2 \lim_{t \rightarrow 0} H_{CC}(t). \quad (\text{A6})$$

An expression for $H_{CC}(t)$ may be derived by Laplace transforming the MSA integral equation (8). After some manipulation we find

- *Permanent address: Laboratoire de Thermodynamique et Physico-Chimie Métallurgiques, Ecole Normale Supérieure d'EEG, Domaine Universitaire, Boîte Postale No. 75, F-38402 Saint-Martin d'Hères, France.
- ¹W. van der Lugt and W. Gertsma, *J. Non-Cryst. Solids* **61-62**, 187 (1984).
 - ²J. Hafner, *J. Non-Cryst. Solids* **61-62**, 175 (1984).
 - ³V. Heine and D. Weaire, in *Solid State Physics, Advances in Research and Application*, edited by H. Ehrenreich, D. Turnbull, and F. Seitz (Academic, New York, 1970), Vol. 24, p. 247.
 - ⁴J. Hafner, *Z. Phys. B* **22**, 351 (1975); **24**, 41 (1976).
 - ⁵M. Rasolt and R. Taylor, *Phys. Rev. B* **11**, 2717 (1975).
 - ⁶J. E. Inglesfield, in *Computer Simulation of Solids*, edited by C. R. A. Catlow and W. C. Mackerodt, Vol. 166 of *Lecture Notes in Physics* (Springer, Berlin, 1982), p. 115.
 - ⁷J. Hafner, in *Amorphous Solids and the Liquid State*, edited by N. H. March, R. A. Street, and M. P. Tosi (Plenum, New York, 1985), p. 91.
 - ⁸*The Liquid State of Matters: Fluids, Simple and Complex*, edited by E. W. Montroll and J. L. Lebowitz (North-Holland, Amsterdam, 1982), p. 175.
 - ⁹G. Jacucci, I. R. McDonald, and R. Taylor, *J. Phys. F* **8**, L121 (1978).
 - ¹⁰M. J. Huyben, W. van der Lugt, W. A. M. Reimer, J. Th. de Hosson, and C. van Dijk, *Physica* **97B&C**, 338 (1979).
 - ¹¹G. Jacucci, M. Ronchetti, and W. Schirmacher in *Proceedings of the Third International Conference on the Structure of Non-Crystalline Materials*, edited by Ch. Janot (Les Editions de Physique, Paris, in press).
 - ¹²A. Isihara, *J. Phys. 1*, 539 (1968); T. Lukes and R. Jones, *ibid.* **1**, 29 (1968).
 - ¹³W. H. Young, in *Liquid Metals 1976*, edited by R. Evans and D. Greenwood (Institute of Physics, Bristol, 1977), Vol. 30, p. 1.
 - ¹⁴J. Hafner, *Phys. Rev. A* **16**, 351 (1977).
 - ¹⁵A. P. Copestake, R. Evans, and M. M. Telo da Gama, *J. Phys. (Paris) Colloq.* **41**, C8-145 (1980).
 - ¹⁶A. P. Copestake and R. Evans, in *Proceedings of the International Conference on Ionic Liquids, Molten Salts, and Polyelectrolytes*, Vol. 172 of *Lecture Notes in Physics*, edited by K. H. Bennemann and D. Quitmann (Springer, Berlin, 1982), p. 86.
 - ¹⁷A. P. Copestake, R. Evans, H. Ruppertsberg, and W. W. Schirmacher, *J. Phys. F* **13**, 1993 (1983).
 - ¹⁸E. Waisman, *J. Chem. Phys.* **59**, 495 (1973).
 - ¹⁹J. Hafner, A. Pasturel, and P. Hicter, *J. Phys. F* **14**, 1137 (1984); **14**, 2279 (1984).
 - ²⁰J. Hafner, A. Pasturel, and P. Hicter, *Z. Metallkd.* **76**, 432 (1985).
 - ²¹J. Hafner, *J. Phys. F* **6**, 1243 (1976).
 - ²²J. Hafner, *Phys. Rev. B* **15**, 617 (1977).
 - ²³J. Hafner, *Phys. Rev. B* **21**, 406 (1980).
 - ²⁴D. R. Hamann, M. Schlüter, and C. Chiang, *Phys. Rev. Lett.* **43**, 1494 (1979).
 - ²⁵G. B. Bachelet, D. R. Hamann, and M. Schlüter, *Phys. Rev. B* **26**, 4199 (1982).
 - ²⁶M. H. Cohen and V. Heine, *Phys. Rev.* **122**, 1821 (1961).
 - ²⁷L. Pauling, *The Nature of the Chemical Bond*, 2nd ed. (Cornell University Press, Ithaca, 1952), Sec. 12.5.
 - ²⁸W. Biltz and F. Weibke, *Z. Anorg. Chem.* **223**, 321 (1935).
 - ²⁹J. Hafner and V. Heine, *J. Phys. F* **13**, 2479 (1983); *ibid.* (to be published).
 - ³⁰A. B. Bhatia and D. E. Thornton, *Phys. Rev. B* **2**, 3004 (1970).
 - ³¹M. S. Wertheim, *Phys. Rev. Lett.* **10**, 321 (1963).
 - ³²N. W. Ashcroft and J. Lekner, *Phys. Rev.* **145**, 83 (1966).
 - ³³N. F. Carnahan and K. E. Starling, *J. Chem. Phys.* **51**, 635 (1969).
 - ³⁴See, e.g., B. Hafskjöld and G. Stell, in *The Liquid State of Matter: Fluids, Simple and Complex*, E. W. Montroll and J. L. Lebowitz (North-Holland, Amsterdam, 1982), pp. 175ff.
 - ³⁵Ch. Holzhey, J. R. Franz, and F. Brouers, *J. Phys. F* **14**, 2475 (1984).
 - ³⁶J. Hafner, *Phys. Rev. B* **27**, 678 (1983).
 - ³⁷H. Jones, *J. Chem. Phys.* **55**, 2640 (1971). Note that the original reference contains a misprint.
 - ³⁸H. Rudin, S. Jost, and H. J. Güntherodt, *J. Non-Cryst. Solids* **61-62**, 291 (1984).
 - ³⁹E. Nassif, P. Lamparter, W. Sperl, and S. Steeb, *Z. Naturforsch.* **38a**, 142 (1983).
 - ⁴⁰M. Ito, H. Jwasaki, N. Shiotami, W. Shiotami, H. Narumi, T. Mizoguchi, and T. Kawamura, *J. Non-Cryst. Solids* **61-62**, 303 (1984).
 - ⁴¹J. Hafner, *J. Phys. C* **16**, 5773 (1983).
 - ⁴²P. Chieux and H. Ruppertsberg, *J. Phys. (Paris) Colloq.* **41**, C8-321 (1980).
 - ⁴³H. Ruppertsberg (private communication).
 - ⁴⁴F. Sommer, *Z. Metallkd.* **70**, 359 (1979).
 - ⁴⁵M. L. Saboungi and C. C. Hsu, *CALPHAD* **1**, 237 (1977).
 - ⁴⁶H. Ruppertsberg and W. Speicher, *Z. Naturforsch.* **31a**, 47 (1976).
 - ⁴⁷H. Ruppertsberg and H. Reiter, *J. Phys. F* **12**, 1311 (1982).
 - ⁴⁸M. L. Saboungi, J. Marr, and M. Blander, *J. Chem. Phys.* **68**, 1375 (1978).
 - ⁴⁹H. Ruppertsberg and W. Schirmacher, *J. Phys. F* **14**, 2787 (1984).
 - ⁵⁰V. T. Nguyen and J. E. Enderby, *Philos. Mag.* **35**, 1013 (1977).
 - ⁵¹P. G. de Gennes, *J. Phys. (Paris)* **23**, 630 (1962).